



## Final Results from the Palo Verde Neutrino Oscillation Experiment

A. PIEPKE for the PALO VERDE COLLABORATION

*Department of Physics and Astronomy, University of Alabama, Tuscaloosa, AL 35487, USA*

*December 4, 2001*

### Abstract

The Palo Verde neutrino oscillation experiment, located at 750 and 890 m distance from the three reactors of the Palo Verde nuclear generating station, has collected data for a total of 350 days, 108 days with one of the reactors off for refueling. The neutrino signal and background were determined in two independent ways. The observed  $\bar{\nu}_e$ -flux is consistent with the absence of neutrino oscillations.  $\bar{\nu}_e \leftrightarrow \bar{\nu}_x$  oscillations are excluded, at the 90% c.l., for  $\Delta m^2 > 1.1 \cdot 10^{-3} \text{ eV}^2$ , at full mixing, and  $\sin^2 2\theta < 0.17$  at large  $\Delta m^2$ . The experiment has been concluded, the detector dismantled.

## 1 Introduction

The Palo Verde and Chooz reactor neutrino oscillation searches were motivated by the observation of an anomalous atmospheric neutrino flux ratio  $\nu_\mu/\nu_e$ , by several independent experiments [1, 2, 3]. This finding had been interpreted either through  $\nu_\mu \leftrightarrow \nu_e$  or  $\nu_\mu \leftrightarrow \nu_\tau$  oscillations. The neutrino mass-mixing parameters suggested by these observations are in the range of  $10^{-1} \text{ eV}^2 > \Delta m^2 > 10^{-3} \text{ eV}^2$  and  $\sin^2 2\theta > 0.5$ , for two flavor oscillations.

The probability for neutrinos of energy  $E_\nu$  (MeV), emitted in flavor state  $a$  to be detected in a different flavor state  $b$  is, for two flavor oscillations, given by the well known relation:

$$P(\nu_a \rightarrow \nu_b) = \sin^2 2\theta \sin^2 \frac{1.27 \Delta m^2 L}{E_\nu}, \quad (1)$$

where  $L$  (m) is the distance from the source to the detector and  $\Delta m^2$  ( $\text{eV}^2$ ) is the difference of the squared masses of the mass eigenstates involved. The cross section weighted mean energy of electron anti-neutrinos, emitted by nuclear reactors, is with  $\langle E_\nu \rangle = 4.2 \text{ MeV}$  relatively small. A baseline of  $L \sim 1 \text{ km}$  is adequate to study the  $\Delta m^2$  range suggested by atmospheric neutrinos. Reactors are a source of pure  $\bar{\nu}_e$ . For detection reactions involving the charged current the low energy makes appearance of charged Leptons, other than positrons, impossible. One is hence restricted to a  $\bar{\nu}_e \leftrightarrow \bar{\nu}_x$  disappearance search which only probes the  $\nu_\mu \leftrightarrow \nu_e$  solution to the atmospheric neutrino anomaly, in its original form.

The  $\bar{\nu}_e$  yield and spectra of reactors are well understood from previous experiments [4]. As oscillation signature one can use a comparison of the measured and expected neutrino interaction rate but has to perform an absolute measurement. A near detector is not required. The mixing angle sensitivity is

limited by the statistical accuracy of the measured rate.

Two independent experiments have been performed to search for neutrino oscillations at a distance of about 1 km from nuclear reactors. With  $L/\langle E_\nu \rangle \sim 200$  m/MeV these were the first dedicated “long baseline” experiments. Both the Palo Verde [5] and the Chooz [6] experiment were able to exclude  $\nu_\mu \leftrightarrow \nu_e$  oscillations as the dominant mechanism for the atmospheric neutrino anomaly. This confirms newer Super-Kamiokande results clearly favoring  $\nu_\mu \leftrightarrow \nu_\tau$  oscillations [7].

## 2 Experimental Procedure

The Palo Verde nuclear generating station consists of three identical pressurized water reactors with a thermal power of 11.63 GW each. The neutrino detector was situated 750 m from one of them and 890 m from the two others. To suppress the cosmic radiation the detector was located in a shallow underground lab with an overburden of about 32 mw.e.. While this depth sufficed to eliminate the hadronic component of the cosmic radiation the muon flux was with  $22 \text{ m}^{-2}\text{s}^{-1}$  still relatively high, resulting in a substantial production of tertiary neutrons in the laboratory walls.

As neutrino detection reaction we utilized inverse beta decay:



offering both a “high” cross section (at our energies about  $6 \cdot 10^{-43} \text{ cm}^2/\text{fission}$ ) and convenient active target material in form of hydrogen rich liquid scintillator. The reaction threshold is with 1.8 MeV relatively low. The utilization of the capture of the reaction neutron allows to make use of a delayed coincidence counting scheme, greatly reducing the background. The anti-neutrino target consisted of 11.3 tons of 0.1% Gd loaded liquid scintillator, which had been developed for this experiment [8]. The high thermal neutron cross section of Gd resulted in a tight positron-neutron correlation time of  $\tau_{\text{cap}} = 28 \mu\text{s}$ . Furthermore Gd releases a 8 MeV gamma cascade after neutron capture, giving a robust capture tag.

Figure (1) depicts the detector. The target was contained in 66 9 m long acrylic tanks, viewed by two low background 5” PMTs at either end. These were separated though a passive oil buffer from the active detector to reduce background. The detector segmentation allowed a two dimensional vertex reconstruction, with the third dimension determined by the different arrival times of the scintillation light at the PMTs. On the trigger level a neutrino candidate event required three tanks to fire in a fast coincidence. One “high” hit (more than  $\sim 0.6$  MeV energy deposit in the center of any cell) was associated with the kinetic energy of the reaction positron. Two “low” hits (more than  $\sim 0.05$  MeV energy deposit in the center of the cell) had to occur in adjacent cells, flagging the annihilation radiation. The differences in event topology for annihilation-like and background events allowed an active on-line background rejection. Two triple events within  $450 \mu\text{s}$  of each other would initiate event readout for off-line analysis. A smart, field programmable event trigger was used [9].

The central detector was surrounded by a 1 m thick water buffer, reducing both the ambient gamma ray and neutron flux. The set up was housed in a tight  $4\pi$  veto, build from large liquid scintillation tanks, most of which had been obtained from the MACRO experiment. The veto inefficiency was measured to be  $2.5 \pm 0.2\%$  and  $0.07 \pm 0.02\%$  for stopping and through going muons, respectively.

Stable detector operation was verified through weekly calibrations with light flashers. The energy scale was defined using  $^{22}\text{Na}$  and AmBe sources. Cross checks were provided through runs with  $^{65}\text{Zn}$ ,  $^{137}\text{Cs}$  and  $^{228}\text{Th}$  sources. The positron and neutron detection efficiencies were determined by means of Monte Carlo simulation. This is a central point for an experiment based on the absolute determination of the neutrino flux. Great care was taken to tune these calculations through repeated measurements with various calibration sources. Light attenuation effects were calibrated several time over the life of the experiment by performing 3-dimensional source scans over the whole detector volume using the  $^{228}\text{Th}$

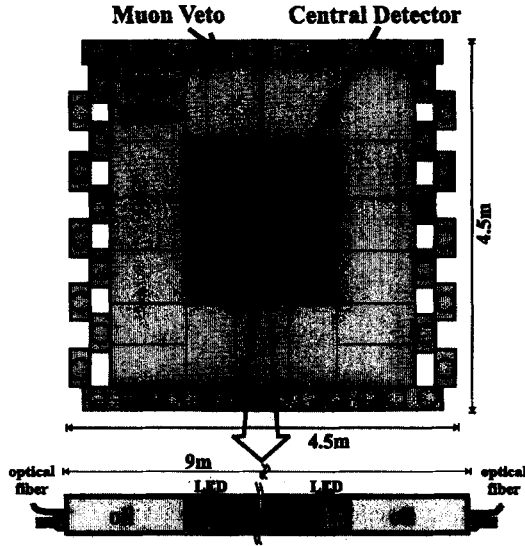


Figure 1: The Palo Verde detector. One of the 66 target cells, with its optical calibration devices, is shown lengthwise at the bottom.

source. Our scintillator exhibited good stability towards aging. All experimental details have been published [5] and will therefore not be repeated here. Data was taken in “runs”, typically lasting a day. The expected anti-neutrino candidate rate  $R_{calc}$  is given by:

$$R_{calc} = n_p \int dE_\nu \sigma(E_\nu) \eta(E_\nu) \times \sum_{i=1}^3 \frac{\Phi_i(E_\nu) [1 - P_{osc,i}(\Delta m^2, \sin^2 2\theta, L_i, E_\nu)]}{4\pi L_i^2}, \quad (3)$$

where  $\sigma(E_\nu)$  is the differential cross section taken from [10],  $\Phi_i(E_\nu)$  the neutrino spectrum emitted by reactor  $i$  at distance  $L_i$ ,  $\eta(E_\nu)$  the energy dependent detection efficiency and  $n_p$  is the number of free protons in the target. The fuel burn-up enters through the evolution of  $\Phi_i(E_\nu)$  into the calculation. Our model was based on a daily log of the thermal reactor power and the fission rates of the nuclides  $^{239}\text{Pu}$ ,  $^{241}\text{Pu}$ ,  $^{235}\text{U}$  and  $^{238}\text{U}$ . The two flavor neutrino oscillation probability  $P_{osc,i}$  was taken as defined in equation (1). Figure (2) shows our  $\bar{\nu}_e$  reaction yield model covering the duration of the experiment.

### 3 Results

The on-line rate of correlated events was about  $1 \text{ s}^{-1}$  with a raw triple event rate of  $50 \text{ s}^{-1}$ . The following off-line cuts were applied to the data to arrive at the final  $\bar{\nu}_e$ -candidate data set:

1. At least one hit was reconstructed with  $E > 1 \text{ MeV}$  in both prompt and delayed *triples* and at least two additional hits showed  $E > 30 \text{ keV}$ . No single hit was allowed to be greater than  $8 \text{ MeV}$ .
2. The prompt *triple* was required to resemble a positron, i.e. annihilation  $\gamma$ 's each less than  $600 \text{ keV}$ , and together less than  $1.2 \text{ MeV}$ . (This cut was the only one which treated the two *triples* asymmetrically).

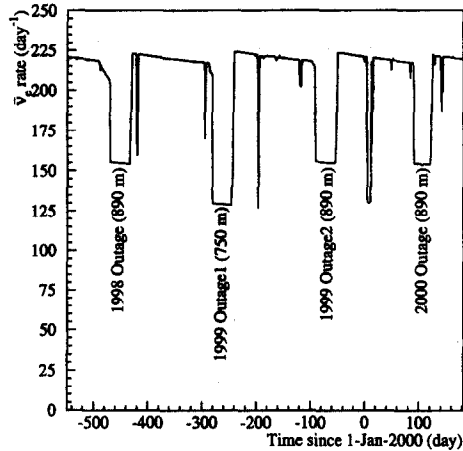


Figure 2: Calculated  $\bar{\nu}_e$  interaction rate in the target for the case of no oscillations. The periods of reduced rate correspond to the refueling outages. The rate variations at full power are due the fuel burn up.

3. At least one of the two *triples* in the event had more than 3.5 MeV of reconstructed energy for rejection of  $\gamma$  backgrounds.
4. The prompt and delayed portions of the event were correlated in space and time (within 3 columns, 2 rows, one meter longitudinally, and 200  $\mu\text{s}$ ).
5. The event started at least 150  $\mu\text{s}$  ( $\sim 5$  neutron capture times) after the previous veto tagged muon activity.

Application of these selection criteria reduced the rate to a more manageable 50 events per day. The neutrino analysis has to unfold the neutrino signal from the background. Correcting this rate by the detection efficiency of about 11% (see table (1)) yields a rate of  $440 \text{ d}^{-1}$ , which clearly exceeds the maximum expected neutrino signal of  $225 \text{ d}^{-1}$  (see figure (2)) without oscillations. A reliable background determination is hence crucial to derive a physics result.

The detector background was composed of two components:

1. Random coincidences mainly caused by radioactivity. It can be measured together with the neutrino signal through events with very long delay time between primary and secondary sub-signal. The hardware cut-off for the inter-event time of 450  $\mu\text{s}$  corresponded to about 16 neutron capture times, it was hence long enough to allow determination of the random background to be:  $4.1 \pm 0.2 \text{ d}^{-1}$ .
2. The principal source of background were fast neutrons which created the primary event through proton recoil and eventually captured. These were true correlated events. Multiple neutrons also significantly contributed to the background. This was demonstrated by the observation that the capture time for events correlated with activity in the veto detector showed a shorter correlation time than expected. The Palo Verde data was used to determine the production rate of tertiary muon induced neutrons at shallow overburden [11].

Table 1: Data taking periods, efficiencies (including lifetime, labeled eff.), measured event rates, and results of the *swap* analysis (see text), including the various background estimates. Uncertainties are statistical only.

Period Reactor	1998		1999-I		1999-II		2000	
	on	890 m off	on	750 m off	on	890 m off	on	890 m o
time (d)	30.4	29.4	68.2	21.8	60.4	29.6	83.2	27.5
eff. (%)	8.0	8.0	11.5	11.6	11.6	11.6	10.9	10.8
measured rates ( $\text{d}^{-1}$ )								
$R_1$	$39.6 \pm 1.1$	$34.8 \pm 1.1$	$54.9 \pm 0.9$	$45.1 \pm 1.4$	$54.2 \pm 0.9$	$49.4 \pm 1.3$	$52.9 \pm 0.8$	$43.1 \pm 1$
$R_2$	$25.1 \pm 0.9$	$21.8 \pm 0.9$	$33.4 \pm 0.7$	$32.0 \pm 1.2$	$32.5 \pm 0.7$	$32.6 \pm 1.0$	$30.2 \pm 0.6$	$30.4 \pm 1$
$(1 - \epsilon_1)B_{\text{pp}}$	0.88	0.89	1.11	1.11	1.11	1.11	1.07	1.07
efficiency corrected rates ( $\text{d}^{-1}$ )								
Backgr.	$292 \pm 11$	$255 \pm 10$	$265 \pm 6$	$266 \pm 10$	$256 \pm 6$	$265 \pm 9$	$249 \pm 5$	$272 \pm 1$
$R_{\nu}$	$202 \pm 19$	$182 \pm 18$	$212 \pm 10$	$124 \pm 17$	$214 \pm 11$	$161 \pm 15$	$237 \pm 10$	$129 \pm 1$
$R_{\text{calc}}$	216	154	218	129	220	155	218	154

The data is summarized in table (1) which lists the observed event rates  $R_1$ , grouped into 8 periods (defined by the reactor power schedule) to reduce the statistical fluctuations. The event rates at reduced power are clearly lower than those recorded at full power.

### 3.1 Reactor Power Analysis

This is the “classical” way to extract the modulated neutrino signal from a constant background. The critical point is to show that the background was in fact constant in time. This was verified by reversing some of the selection cuts in order to obtain high statistics background data sets. These allowed to study the temporal behavior of various background components and confirmed a stable background. Figure (3) shows the measured dead time and neutrino efficiency corrected event rates  $R_{\text{exp}}$ , plotted versus the neutrino signal rate expected for no oscillations. If the data were consistent with no oscillations and the background were constant, then the points should lie along a straight line with unity slope. The intercept can be interpreted as the background scaled by the  $\bar{\nu}_e$  detection efficiency. The fit of a straight line to the data yields a slope of  $1.011 \pm 0.104^{\text{stat}}$  at a reduced  $\chi^2$  of 0.89. The statistical significance of the observed  $\bar{\nu}_e$  signal is  $9.7\sigma$ . The data is in fact consistent with the hypothesis of no oscillations. The background derived from this fit is  $257.5 \pm 20.7^{\text{stat}} \text{d}^{-1}$ .

To construct the confidence area in the  $\Delta m^2 - \sin^2 2\theta$  plane we performed a  $\chi^2$  analysis. Let  $R_{\text{obs},i}$  be the event rate, and  $\sigma_i$  its statistical error, measured in run  $i$ . Let  $B$  be the background rate and  $\alpha$  an overall normalization, bound by the systematic uncertainty  $\sigma_{\text{sys}}$ , estimated to be 0.061. We define the test statistic  $\chi^2$  as:

$$\chi^2(\alpha, B, \Delta m^2, \sin^2 2\theta) = \sum_i \frac{(\alpha R_{\text{calc},i}(\Delta m^2, \sin^2 2\theta) + B - R_{\text{obs},i})^2}{\sigma_i^2} + \frac{(\alpha - 1)^2}{\sigma_{\text{sys}}^2}. \quad (4)$$

The following analysis was based on the data binned as shown in table (1). A run-by-run analysis gave comparable results.

$\chi^2$  was minimized with regards to  $\alpha$ ,  $B$ ,  $\Delta m^2$  and  $\sin^2 2\theta$  on a fine grid in the  $\Delta m^2 - \sin^2 2\theta$  plane. The best fit obtained was identical to the no oscillation fit ( $\Delta m^2 = \sin^2 2\theta = 0$ ) consistent with the absence of neutrino oscillations.

The 90% c.l. acceptance region is defined according to the procedure suggested by Feldman and Cousins [12] by determining the change in  $\chi^2$  during the grid search:

$$\Delta\chi^2 = \chi^2(\Delta m^2, \sin^2 2\theta) - \chi_{\text{best}}^2 > \Delta\chi_{\text{crit}}^2(\Delta m^2, \sin^2 2\theta) \quad (5)$$

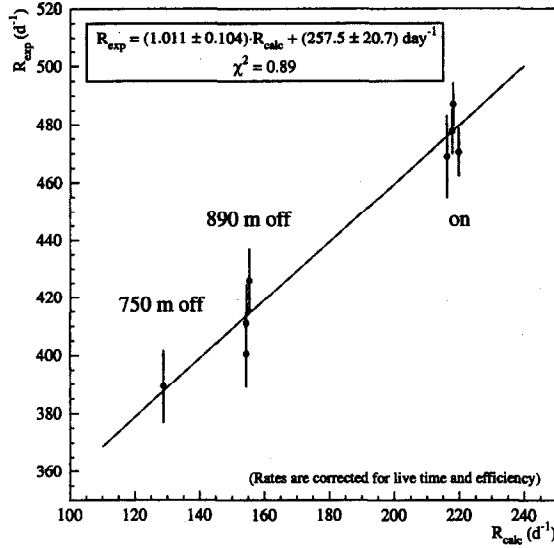


Figure 3: The event rates  $R_{\text{exp}}$  for different data taking periods, corrected for dead time and neutrino detection efficiency, plotted versus the expected neutrino interaction rate  $R_{\text{calc}}$  for no oscillations. Errors are statistical only. Points corresponding to data taking periods with the same reactor power conditions should lie on top of each other. Also shown is the result, discussed in the text, of a linear fit to the data.

where  $\chi^2(\Delta m^2, \sin^2 2\theta)$  is the minimized fit quality at the current point in the  $\Delta m^2 - \sin^2 2\theta$  plane. Clearly a large  $\Delta\chi^2$  indicates a big deviation from the best fit and therefore signals disagreement with the data. Quantitatively  $\Delta\chi^2_{\text{crit}}$ , the  $\chi^2$  acceptance cutoff at the given c.l., was obtained through Monte Carlo simulation.

This procedure is rather time consuming and cumbersome. An alternate construction of the confidence area used the so called raster scan. In this analysis a global best fit is not constructed but  $\sin^2 2\theta$  is minimized for fixed  $\Delta m^2$  instead. This is repeated for each  $\Delta m^2$  value of interest. The confidence region is then the union of all *one dimensional* confidence intervals calculated. The unified analysis [12] is now much simplified as we are only dealing with a one dimensional problem. The exclusion plot labeled “reactor power” in figure (4) was based on a raster scan. The full Monte Carlo analysis delivered a nearly identical result.

### 3.2 The Swap Analysis

In the “swap analysis” most of the background is directly subtracted rather than using the information on the reactor power. It has therefore a substantially greater statistical power and a different systematics, at the expense of a somewhat stronger reliance on the Monte Carlo simulation. A detailed description of the method has been published [13].

Let  $R_1$  be the observed event rate after applying the neutrino selection cuts, let  $R_2$  be the rate obtained when applying the neutron cuts to the positron like sub-event and the positron selection cuts to the neutron like sub-event (“swapped” selection). In the difference  $R_1 - R_2$  the two-neutron and

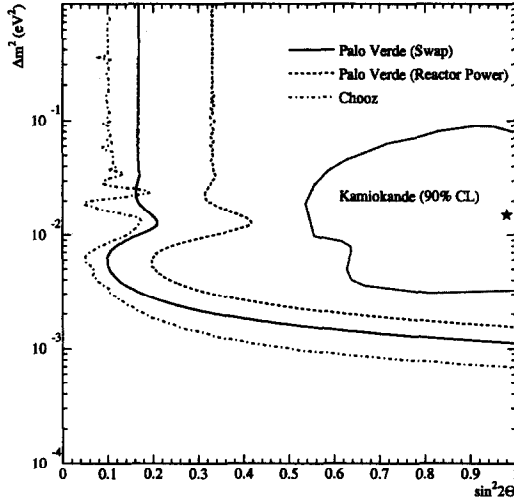


Figure 4:  $\Delta m^2 \sin^2 2\theta$  exclusion plot. The 90% c.l. limits obtained by the “reactor power” (dashed line) and the “swap” (solid line) analysis are shown in comparison to the Chooz [6] exclusion and the allowed parameter range of the original Kamiokande experiment [1].

random backgrounds cancel, while only 20% of the anti-neutrino signal cancels. The contribution of the proton-neutron scattering background is given by  $(1 - \epsilon_1)B_{pn}$ . It is dominated by neutrons created in muon spallation in the laboratory walls and muon capture inside the detector. While neutron production through muon capture is well understood and can be reliably calculated through Monte Carlo simulation, the spallation is rather poorly known. The spectral shape of the spallation neutrons was obtained by Monte Carlo using several parametric models selected to span the range of uncertainty in our knowledge of the energy dependence of neutron production. The normalization was then obtained by assuming that all events with a prompt energy of greater than 10 MeV are exclusively due to spallation. The dispersion between the different neutron flux models was taken into account in the systematic error. The quantity  $(1 - \epsilon_1)B_{pn}$  was then determined period by period. Its magnitude is small compared to  $R_1 - R_2$  so that its contribution to the background largely cancels in the difference. Therefore even a systematic uncertainty of 100% in  $(1 - \epsilon_1)B_{pn}$  results in only a few percent contribution to the error of the neutrino signal. Table (1) lists the quantities relevant in the swap analysis period by period. Similarly to the reactor power analysis, we have carried out a  $\chi^2$  analysis to test our data for oscillations throughout the  $\Delta m^2 - \sin^2 2\theta$  plane. The  $\chi^2$  definition was:

$$\chi^2(\alpha, \Delta m^2, \sin^2 2\theta) = \sum_{i=1}^8 \frac{(R_{1,i} - R_{2,i} - (1 - \epsilon_1)B_{pn} - \alpha(R_{\text{calc}}^{1,i} - R_{\text{calc}}^{2,i}))^2}{\sigma_i^2} + \frac{(\alpha - 1)^2}{\sigma_{\text{sys}}^2} \quad (6)$$

where  $\sigma_{\text{sys}}$  for the “swap” method is estimated to be 0.053 as discussed below. The free parameters in this definition of the  $\chi^2$  are  $\Delta m^2$ ,  $\sin^2 2\theta$ , and  $\alpha$ . The Monte Carlo method gives  $\chi_{\text{best}}^2/d.o.f. = 10.3/7$  for  $\sin^2 2\theta$  consistent with zero and a slightly un-physical  $\alpha = 1.008$ .

The region of parameter space excluded at the 90% c.l. by this analysis, based on the raster scan

method, is indicated by the solid curve in Fig. (4). In the limit of large  $\Delta m^2$ , the range  $\sin^2 2\theta > 0.168$  is excluded; whereas in the limit of large mixing, the range  $\Delta m^2 > 1.1 \times 10^{-3} \text{ eV}^2$  is excluded. We note that, in the limit of large  $\Delta m^2$ , the Monte Carlo method excludes the range  $\sin^2 2\theta > 0.165$ , and gives an essentially identical exclusion curve.

The systematic uncertainty has contributions from the detection efficiency, the flux calculations. The

Table 2: Contributions to the systematic error of the “reactor power” and “swap” analyses.

Error source	“reactor power” (%)	“swap” (%)
$e^+$ trigger efficiency	2.0	2.0
n trigger efficiency	2.1	2.1
$\bar{\nu}_e$ flux prediction	2.1	2.1
$\bar{\nu}_e$ selection cuts	4.5	2.1
Background variation	2.1	N/A
$(1 - \epsilon_1)B_{\text{pn}}$ estimate	N/A	3.3
<b>Total</b>	<b>6.1</b>	<b>5.3</b>

“reactor power” method suffers a systematic error from possible background variations in time, while the “swap” analysis has an error contribution from the estimate of  $(1 - \epsilon_1)B_{\text{pn}}$ . The individual contributions are shown in Table 2 and were added in quadrature to obtain the total systematic error for each analysis method.

The analysis of the energy distribution of the neutrino candidate events provides an addition oscillation

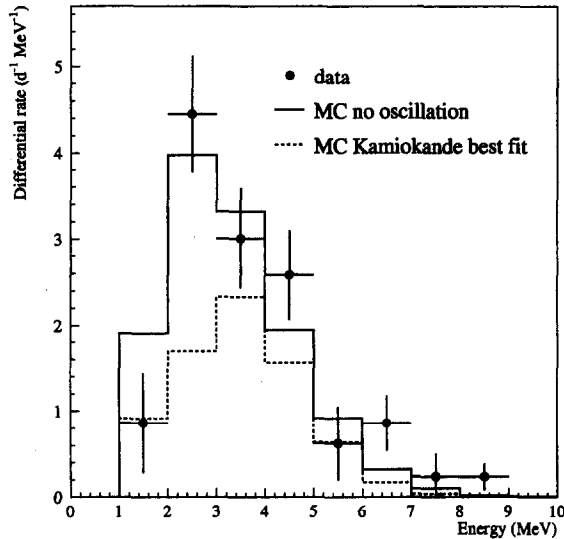


Figure 5: Prompt energy spectrum after *on-off* subtraction. The histograms show the expectations for no oscillation (solid line) and Kamiokande best fit (dashed line).

check. For each of the pairs of *on-off* periods one may subtract the spectrum taken at partial power from that taken at full power. After a small correction for fuel burn-up, the resulting spectrum is due

to the reactor which has been refueled during the off period. Figure (5) shows the weighted average of all four on-off periods, *without* efficiency and dead time correction. Also shown are the spectra we would have expected based on the Kamiokande [1] best fit for  $\nu_\mu \leftrightarrow \nu_e$  oscillations ( $\chi^2/d.o.f. = 3.69$  for eight degrees of freedom) and no oscillations ( $\chi^2/d.o.f. = 1.39$ ) In agreement with the two previous analysis also the energy spectrum supports the no oscillation hypotheses.

## 4 Conclusion

The Palo Verde data is consistent with the absence of  $\bar{\nu}_e \leftrightarrow \bar{\nu}_x$  oscillations. This conclusion has been derived through two independent analysis techniques. Through the “swap” analysis, yielding the more restrictive bound, we determined the ratio of observed interaction rate to expected to be:  $R_{\text{obs}}/R_{\text{calc}} = 1.01 \pm 0.024^{\text{stat}} \pm 0.053^{\text{sys}}$ . These final results are dominated by systematics errors. Our data exclude two family  $\nu_\mu - \nu_e$  mixing as being responsible for the anomaly reported by Kamiokande [1]. This result confirms those of the Chooz [6] and and Super-Kamiokande [7] experiments.

The Palo Verde Collaboration: F. Boehm, J. Busenitz, B. Cook, G. Gratta, H. Henrikson, J. Kornis, D. Lawrence, K.B. Lee, K. McKinney, L. Miller, V. Novikov, A. Piepke, B. Ritchie, D. Tracy, P. Vogel, Y-F. Wang, J. Wolf

## References

- [1] Y. Fukuda et al., *Phys. Lett. B* 335 (1994) 237
- [2] R. Becker-Szendy et al., *Phys. Rev. Lett.* 69 (1992) 1010
- [3] E. Peterson et al., *Nucl. Phys. B Proc. Suppl.* 77 (1999) 111
- [4] G. Zacek et al., *Phys. Rev. D* 34 (1986) 2621  
Y. Declais et al., *Nucl. Phys. B* 434 (1995) 503
- [5] F. Boehm et al., *Phys. Rev. D* 62 (2000) 072002  
F. Boehm et al., *Phys. Rev. D* 64 (2001) 112001
- [6] M. Apollonio et al., *Phys. Lett. B* 466 (1999) 415
- [7] Y. Fukuda et al., *Phys. Rev. Lett.* 81 (1998) 1562  
S. Fukuda et al., *Phys. Rev. Lett.* 85 (2000) 3999
- [8] A. Piepke, S.W. Moser and V.M. Novikov, *Nucl. Inst. Meth. A* 432 (1999) 392
- [9] G. Gratta et al., *Nucl. Inst. Meth. A* 400 (1997) 456
- [10] P. Vogel and J. Beacom, *Phys. Rev. D* 60 (1999) 053003
- [11] F. Boehm et al., *Phys. Rev. D* 62 (2000) 092005
- [12] G. J. Feldman and R. D. Cousins, *Phys. Rev. D* 57 (1998) 3873
- [13] Y.F. Wang et al., *Phys. Rev. D* 62 (2000) 013012